Calmodulin regulates protease versus co-chaperone activity of a metacaspase

Graphical abstract

Highlights

- Metacaspase Mca1 executes cell death and cleaves the Hsp40 co-chaperone Sis1

- Calmodulin inhibits proteolytic activity of Mca1 by binding to its N terminus

- This binding promotes co-chaperone-like activity of Mca1 in Sis1-dependent PQC and longevity

Authors

Anna Maria Eisele-Bürger,
Frederik Eisele, Sandra Malmgren Hill, ...,
F. Ulrich Hartl, Peter V. Bozhkov,
Thomas Nyström

Correspondence

peter.bozhkov@slu.se (P.V.B.),
thomas.nystrom@cmb.gu.se (T.N.)

In brief

Eisele-Bürger et al. report that the dual role of yeast metacaspase Mca1 as a pro- and anti-death factor involves calmodulin binding to its N terminus. This binding inhibits proteolytic activity of Mca1 essential for cell death while enabling its co-chaperone-like activity in Hsp40-dependent proteostasis and longevity.
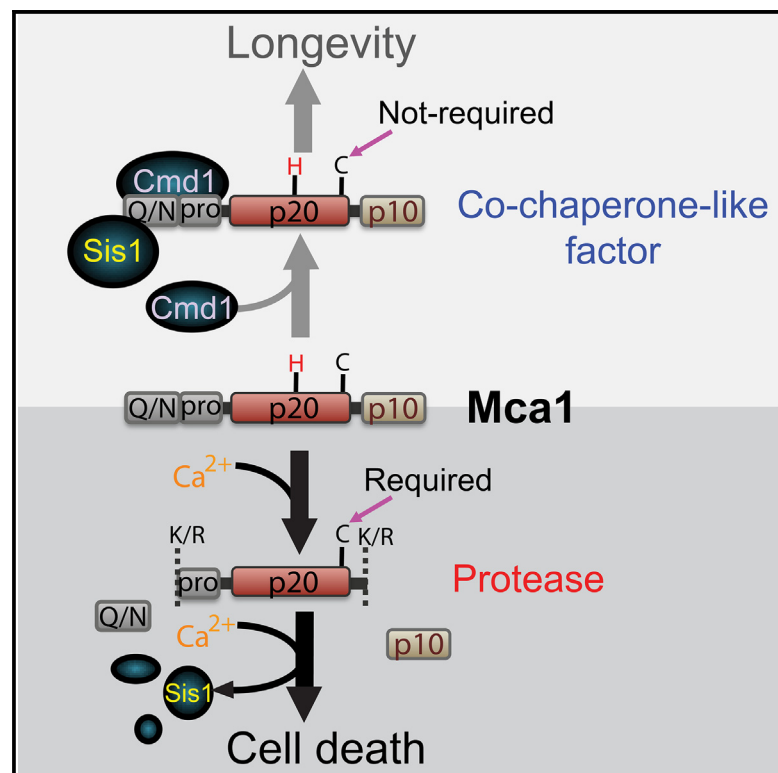
CelPress

Report

Calmodulin regulates protease versus co-chaperone activity of a metacaspase

Anna Maria Eisele-Bürger,[1,2] Frederik Eisele,[1,3] Sandra Malmgren Hill,[1] Xinxin Hao,[1] Kara L. Schneider,[1] Rahmi Imamoglu,[4] David Balchin,[4] Beidong Liu,[3] F. Ulrich Hartl,[4] Peter V. Bozhkov,[2,*] and Thomas Nyström[1,5,*]

[1]Department of Microbiology and Immunology, University of Gothenburg, 40530 Gothenburg, Sweden
[2]Department of Molecular Sciences, Uppsala BioCenter, Swedish University of Agricultural Sciences and Linnean Center for Plant Biology, PO Box 7015, 75007 Uppsala, Sweden
[3]Department of Chemistry and Molecular Biology, University of Gothenburg, Medicinaregatan 9C, 413 90 Göteborg, Sweden
[4]Department of Cellular Biochemistry, Max Planck Institute of Biochemistry, Am Klopferspitz 18, 82152 Martinsried, Germany
[5]Lead contact
*Correspondence: peter.bozhkov@slu.se (P.V.B.), thomas.nystrom@cmb.gu.se (T.N.)
https://doi.org/10.1016/j.celrep.2023.113372

SUMMARY

Metacaspases are ancestral homologs of caspases that can either promote cell death or confer cytoprotection. Furthermore, yeast (*Saccharomyces cerevisiae*) metacaspase Mca1 possesses dual biochemical activity: proteolytic activity causing cell death and cytoprotective, co-chaperone-like activity retarding replicative aging. The molecular mechanism favoring one activity of Mca1 over another remains elusive. Here, we show that this mechanism involves calmodulin binding to the N-terminal pro-domain of Mca1, which prevents its proteolytic activation and promotes co-chaperone-like activity, thus switching from pro-cell death to anti-aging function. The longevity-promoting effect of Mca1 requires the Hsp40 co-chaperone Sis1, which is necessary for Mca1 recruitment to protein aggregates and their clearance. In contrast, proteolytically active Mca1 cleaves Sis1 both *in vitro* and *in vivo*, further clarifying molecular mechanism behind a dual role of Mca1 as a cell-death protease versus gerontogene.

INTRODUCTION

Caspases are a family of cysteine-dependent aspartate-specific proteases, best known for their crucial role in the activation and/or execution of apoptotic cell death in animals.[1,2] Non-animal eukaryotes lack direct homologs of caspases but possess structurally related proteases of bacterial origin called metacaspases.[3–5] Despite similar structural folds, metacaspases and caspases have distinct substrate specificity, with metacaspases strictly requiring arginine and/or lysine in the P1 position of their substrates.[6,7]

In the yeast *Saccharomyces cerevisiae*, Mca1 (also known as Yca1 [yeast caspase-1]) has been shown to act as a positive regulator of cell death,[8] as deletion of the *MCA1* gene or a mutation of the catalytic cysteine (Cys276) abrogated the cell-death phenotype observed in yeast under acute or chronic stress conditions.[9,10] However, *MCA1* deletion also induces intrinsic cellular stress leading to upregulation of many stress response genes encoding, for example, components of the proteasome, DNA-repair systems, and chaperones.[11–13] This indicates that the yeast Mca1 is also bestowed with pro-survival functions. Accordingly, it has been shown that Mca1 localizes to Hsp104-containing cytosolic protein inclusions, IPOD and JUNQ, outside the nucleus and underpins protein quality control (PQC)[14–16] by promoting the clearance of insoluble protein aggregates.[16,17] This proteostatic role of Mca1 is independent of autophagy, as

the autophagosomal marker protein Atg8 is absent from the Hsp104-containing protein inclusions.[18] Thus, ectopic overexpression of Mca1 counteracts the buildup of aggregated proteins during both stress[16,17] and replicative aging[16] and extends lifespan.[16] Furthermore, the positive effects of Mca1 on survival and longevity are independent of its proteolytic activity.[16] Instead, the proteostatic function of Mca1 appears connected to Hsp40 co-chaperone activity, as Mca1 buffers against deficiencies in the yeast Hsp40 co-chaperone Ydj1.[16] In addition, Mca1 interacts physically with another Hsp40, the essential protein Sis1,[19] suggesting that Mca1 and Sis1 may act cooperatively in buffering the Ydj1 system.

Taken together, the available evidence assigns a dual role of the yeast Mca1 that can act both as a protease essential for the execution of regulated cell death and as an important component of PQC for cytoprotection and longevity. Here, we provide a molecular explanation for such a dual role of Mca1 by establishing calmodulin binding as a regulatory switch between the two Mca1 functions. This binding prevents autocatalytic processing and activation of the protease zymogen, switching from pro-death to proteostatic function of Mca1. We further demonstrate that while Hsp40 co-chaperone Sis1 is required for Mca1 to fulfill its role in PQC and lifespan extension, it represents also a proteolytic target of active Mca1 whose cleavage may contribute to the execution of Mca1-dependent cell death.
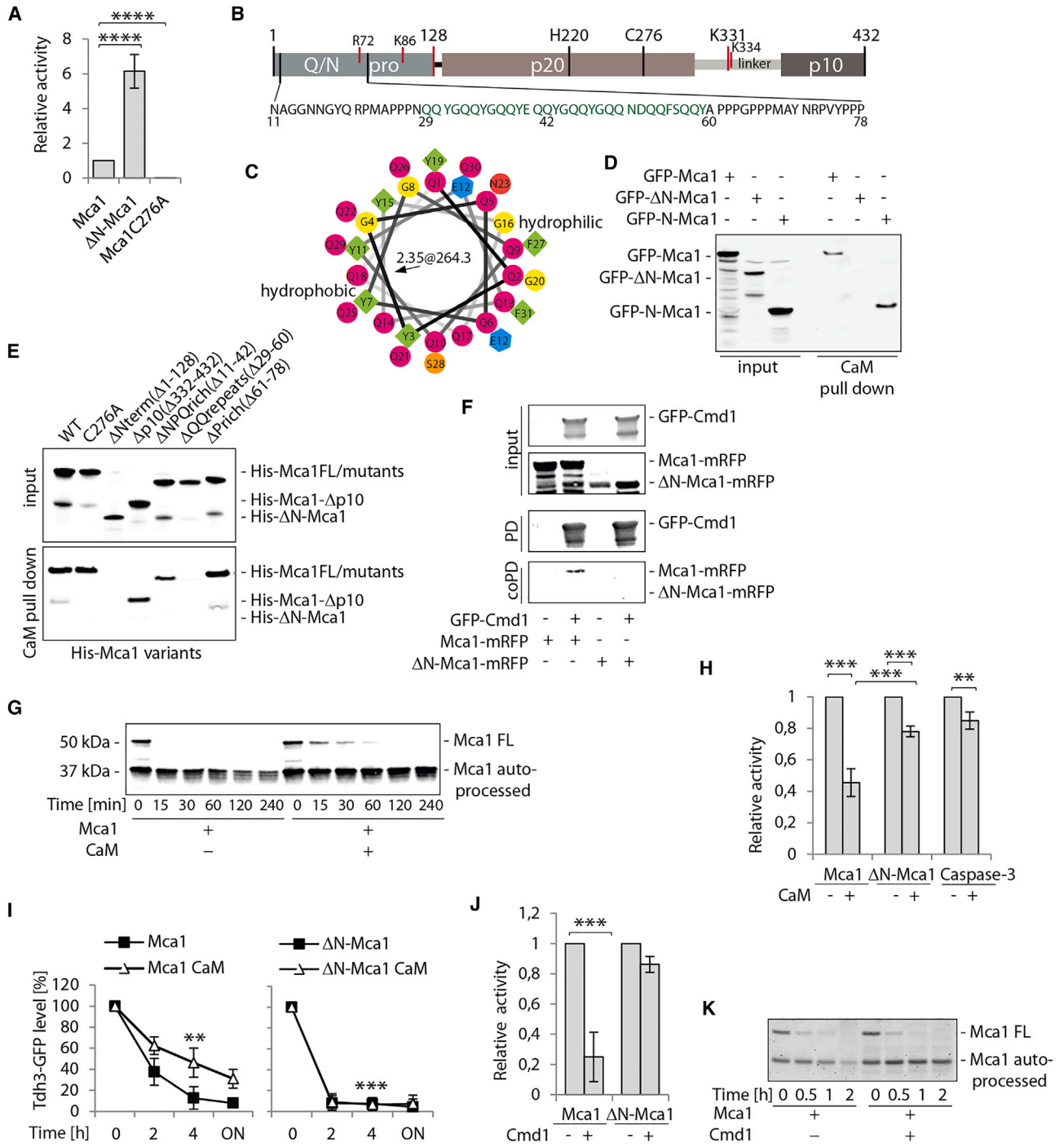
Figure 1. The N-terminal pro-domain of Mca1 modulates proteolytic activity through interaction with calmodulin

(A) Relative proteolytic activity of full-length Mca1, ΔN-Mca1, and Mca1C276A against Ac-VRPR-AMC in the presence of 1 mM $CaCl_2$ (unpaired t test, ****p < 0.0001, n = 2–5 independent experiments).

(B) Domain composition of Mca1 showing the catalytic dyad H220 and C276. The R72, K86, K331, and K334 residues are the putative autocleavage sites for Mca1 activation.[21] The N-terminal pro-domain (pro) includes Q/N-rich and P-rich regions (jointly indicated as Q/N). The calmodulin-binding region is highlighted in green within the amino acid stretch. p20 and p10, p20- and p10-like regions, respectively, separated by a linker.

(C) Helical wheel projection of the putative α-helical amphipathic region of Mca1 residues 29–60, highlighted in green in (B). Arrow indicates hydrophobic region, and 2.35@264.3 indicates helicity and hydrophobic moment (https://www.donarmstrong.com/cgi-bin/wheel.pl).

(D) Interaction of GFP-Mca1, -ΔN-Mca1-, and -N-Mca1 from yeast cell lysates (input) with calmodulin (CaM)-Sepharose beads. Bound proteins were pulled down (PD) with the beads, analyzed by western blot, and visualized with anti-GFP.

(legend continued on next page)

RESULTS

Mca1 is a promiscuous protease

To understand how Mca1 can act as both a cellular executioner and protector, we first revisited its protease function, which was initially connected to cell death,[9,20] by optimizing the protein purification protocol such that we could isolate a catalytically active full-length recombinant metacaspase. Consistent with earlier studies, we found that Mca1 processed itself, in a Ca^{2+}-dependent manner, resulting in several proteoforms (Figure S1A).[19,21] Notably, such Mca1 autoprocessing might be required for proteolytic activation, as shown for type II metacaspases[6,22] and other proteases.[23] Mass spectrometry (MS) analysis revealed multiple autocleavage sites with R or K in the P1 position but no clear preference for amino acids in P2-P4 and P1′-P4′ positions (Figures S1B and S1C). Supporting this notion, we found that randomly selected recombinant proteins, e.g., Sgt2, Mms21, Myo2, and Mon2, were all cleaved by Mca1 (Figure S1D). Since Mca1 displays loose substrate specificity beyond P1, at least *in vitro*, its activity *in vivo* must be tightly regulated to protect the intracellular polypeptides from unspecific proteolysis.

The N-terminal pro-domain of Mca1 modulates its proteolytic activity via calmodulin binding

The crystal structure of Mca1[21] lacks the N-terminal pro-domain, which is natively unstructured, as predicted by AlphaFold (Figure S1E). We found that this region inhibits Mca1 catalysis, as its deletion (generating the ΔN-Mca1 protein) enhanced both autocatalytic processing (see also[17]) and protease activity (Figure 1A). Importantly, parts of the Q-rich N-terminal pro-domain of Mca1 resemble amphipathic regions (Figures 1B and 1C) that have been reported to bind calmodulin.[24–26] Since it has previously been shown that the yeast *S. cerevisiae* calmodulin Cmd1 and Mca1 have similar effects on the asymmetrical inheritance of protein aggregates,[16,27] that Cmd1 is enriched in aged cells,[28] and, finally, that mammalian calmodulin can regulate protease activity of calpain,[29] we embarked on studying whether Cmd1 and Mca1 interact and, if so, if this affects Mca1 activity.

Indeed, we found that the wild-type and catalytically inactive Mca1 as well as p10-deleted Mca1 and a peptide including only the N-terminal 128 amino acids of Mca1 (N-Mca1) could all interact with bovine calmodulin (100% identical with human calmodulin CaM) *in vitro* in a calcium-independent manner (Figures 1D and S2A). In contrast, Mca1 lacking the N-terminal domain did not bind CaM (Figures 1D and S2A). We could narrow the CaM-binding region down to amino acids 29–60 (Figure 1E). In addition, we confirmed that Mca1 interacted with the yeast calmodulin Cmd1 (60% identical to human CaM)[30–32] *in vivo* in an N-terminal-dependent manner (Figure 1F).

By binding the N terminus of Mca1, human CaM significantly inhibited autoprocessing of the full-length Mca1 (Figure 1G) as well as its proteolytic activity against both peptidic substrate (Figure 1H) and the presumed biological substrate Tdh3[33] (Figure 1I). These inhibitory effects of CaM on Mca1 proteolytic activity were significantly suppressed or completely abolished by deletion of the N-terminal domain of Mca1 (Figures 1H and 1I). As a negative control, we used active caspase-3, a distantly related cysteine protease from the same C14 superfamily as metacaspases,[4] and demonstrated only slight inhibition of its aspartate-specific activity against peptidic substrate by CaM, presumably due to unspecific interaction between the two proteins.

To further substantiate inhibitory effect of calmodulin on protease activity of Mca1, we cloned and purified recombinant yeast Cmd1 from *E. coli* and could demonstrate a conserved inhibition of Mca1 activity *in vitro* by different sources of calmodulin (Figures 1J and 1K, cf. Figures 1G–1I). Importantly, calmodulin inhibited proteolytic activity of Mca1 under conditions of 400- to 1,000-fold excess of Ca^{2+} over calmodulin, ruling out the possibility that reduced Mca1 activity was due to titration of Ca^{2+} in these assays. Thus, we conclude that the N terminus of Mca1 represents a negative *cis*-acting modulator of Mca1 activity on its own and allows for further *trans*-acting modulation by calmodulin binding.

Calmodulin prevents cell death by binding the N-terminal pro-domain of Mca1

To determine the possible relevance of yeast calmodulin Cmd1 binding to Mca1 *in vivo*, we performed pull-down experiments to identify mutant Cmd1s (proteins of temperature-sensitive *cmd1* alleles) that failed to interact with Mca1 and found Cmd1-8 (G113V[34,35]) as one such protein (Figure 2A). We observed that Mca1 was increasingly processed in *cmd1-8* mutant cells but remained as a full-length zymogen in wild-type cells (Figure 2B), demonstrating that Cmd1 inhibits autocatalytic cleavage of Mca1 also *in vivo*. Accordingly, we observed increased metacaspase-like (VRPRase) proteolytic activity in cell lysates from the *cmd1-8* mutant compared to lysates from wild-type cells, both overexpressing Mca1 (Figure 2C), thus corroborating inhibition of Mca1 protease activity by calmodulin *in vivo*.

(E) Interaction of recombinant N-terminal Mca1-deletion mutants from *E. coli* cell extracts with CaM-Sepharose beads. Anti-His was used to immunodetect the PD proteins.

(F) *In vivo* interaction between yeast GFP-Cmd1 and Mca1-mRFP or ΔN-Mca1-mRFP. PD proteins were analyzed by immunoblotting with anti-GFP and anti-Mca1.

(G) Autoprocessing of purified Mca1 in the presence or absence of human CaM visualized by immunoblotting with anti-Mca1.

(H) Relative proteolytic activity of Mca1 or ΔN-Mca1 against Ac-VRPR-AMC (n = 7) and of caspase-3 (n = 3) against Ac-DEVD-AMC in the absence or presence of CaM (unpaired t test, **p < 0.05 and ***p < 0.005).

(I) *In vitro* degradation of Tdh3-GFP by Mca1 in the presence or absence of CaM at indicated time points (ON, overnight) (unpaired t test, **p < 0.05 for all time points, n = 3 independent experiments).

(J and K) VRPRase activity (unpaired t test, ***p < 0.0005, n = 3 independent experiments) (J) and autoprocessing (K) of Mca1 in the presence or absence of yeast Cmd1.

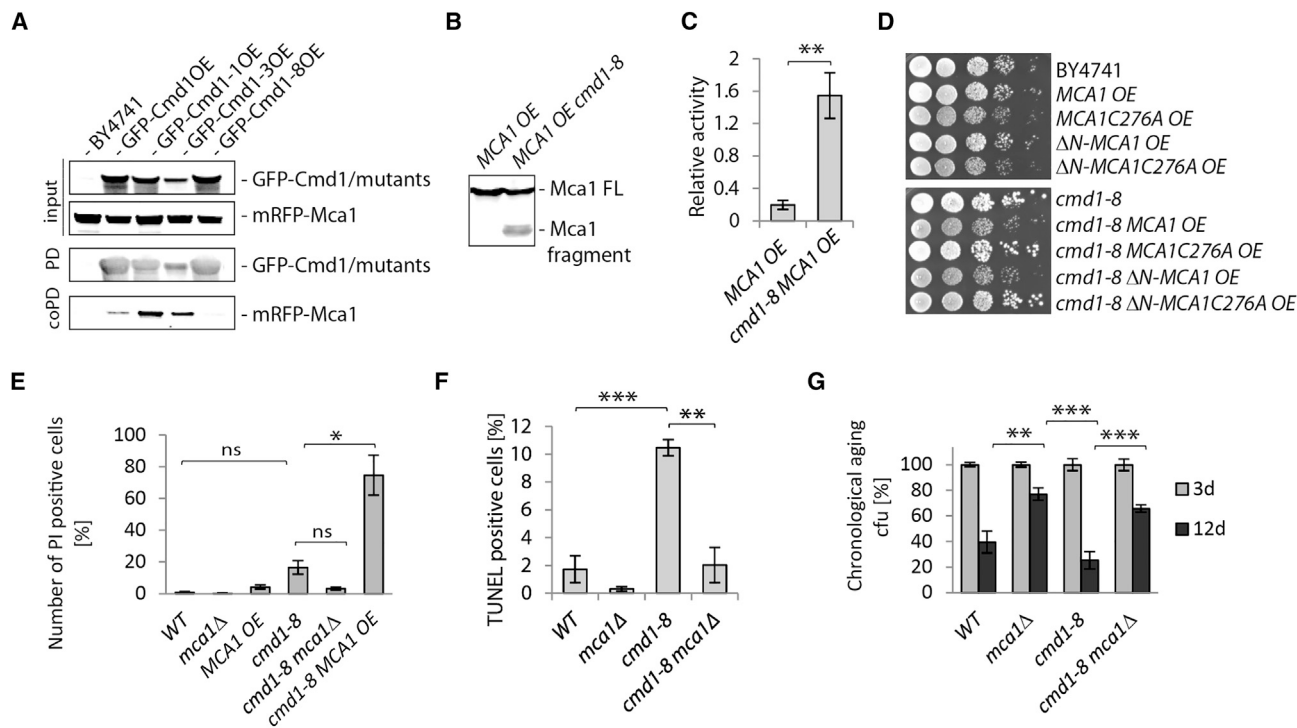Error bars in (A) and (H)–(J) indicate SD. FL, full length.

Figure 2. Calmodulin inhibits Mca1-dependent cell death during chronological aging

(A) Interaction of wild-type and mutant GFP-Cmd1 with Mca1-mRFP in yeast cell extracts (input). GFP-Cmd1 and GFP-Cmd1-1, -3, and -8 mutants were PD from yeast cell extracts (input) containing Mca1-mRFP by using GFP-Trap beads. Proteins were visualized by immunoblotting with anti-GFP and anti-Mca1.

(B) Mca1 fragmentation in cell extracts of wild-type and *cmd1-8* mutant cells overexpressing (OE) Mca1 was visualized by immunoblotting with anti-Mca1. FL, full length.

(C) Relative VRPRase activity in cell extracts of exponentially growing *MCA1* OE and *cmd1-8 MCA1* OE cells (unpaired t test, **p = 0.003).

(D) Exponentially growing cells (optical density 600 [OD_{600}] = 0.5 units/mL) were spotted in serial 10-fold dilution on YPD and incubated at 30°C to monitor growth.

(E) PI staining of dead cells in chronologically aged strains as indicated (unpaired t test, ^{ns}p>0.05, *p < 0.05, n = 2 independent experiments).

(F) DNA fragmentation assessed by TUNEL in exponentially growing wild-type (WT) and *cmd1-8* cells upon *MCA1* deletion (unpaired t test, **p < 0.05 and ***p < 0.005, n = 3 independent experiments).

(G) Clonogenic assay demonstrating increased cell survival upon *MCA1* deletion independent of introducing *cmd1-8* mutation in stationary cells (unpaired t test, **p < 0.01 and ***p < 0.001, n = 2–5 independent experiments). cfu, colony-forming units.

Error bars in (C), (E), and (F) indicate SD while those in (G) indicate SEM.

Overexpression of the constitutively active mutant ΔN-Mca1 and wild-type Mca1 in *cmd1-8* cells retarded proliferation, whereas no such effects were observed by deleting *MCA1* or overexpressing the catalytically inactive mutant Mca1C276A (Figure 2D and S2B), demonstrating that the inhibitory effect on cell proliferation is attributed to the proteolytic function of Mca1.

We further found that the reduced growth of *cmd1-8* cells was, at least in part, a consequence of Mca1-dependent cell death, as the *cmd1-8* cultures displayed an increased proportion of dead cells as judged by propidium iodide (PI) staining (Figure 2E) and by terminal deoxynucleotidyl transferase dUTP nick-end labeling (TUNEL) (Figure 2F). This enhanced cell-death phenotype was reversed by deleting *MCA1* (Figures 2E and 2F), demonstrating the requirement for Mca1 in cell death induced by calmodulin deficiency. We also observed that removing *MCA1* retarded aging of both stationary-phase wild-type and *cmd1-8* cells, which displayed somewhat accelerated aging compared to wild-type cells (Figure 2G). We hypothesize that under chrono-

logical aging conditions, Mca1 may be activated as a protease because calmodulin is titrated out, and such an effect would be even more severe by the inactivation of calmodulin through the *cmd1-8* mutation. In both scenarios, however, it appears that it is the presence of Mca1 that causes the loss of viability. In summary, calmodulin curtails activation of the Mca1 protease by interacting with its N-terminal pro-domain and in this way controls initiation of metacaspase-dependent growth inhibition and cell death.

A constitutively active Mca1 protease fails to extend lifespan and to boost PQC

Since the proteolytic activity appears to be key to the pro-death role of Mca1,[9] we tested if this activity is also linked to its pro-survival function and ability to extend lifespan. We found that while overexpression of wild-type Mca1 led to replicative lifespan extension (as also seen in Hill et al.[16]), the overexpression of the constitutively active ΔN-Mca1 protease failed to do so (Figure 3A). Consistently, and in line with the previously shown
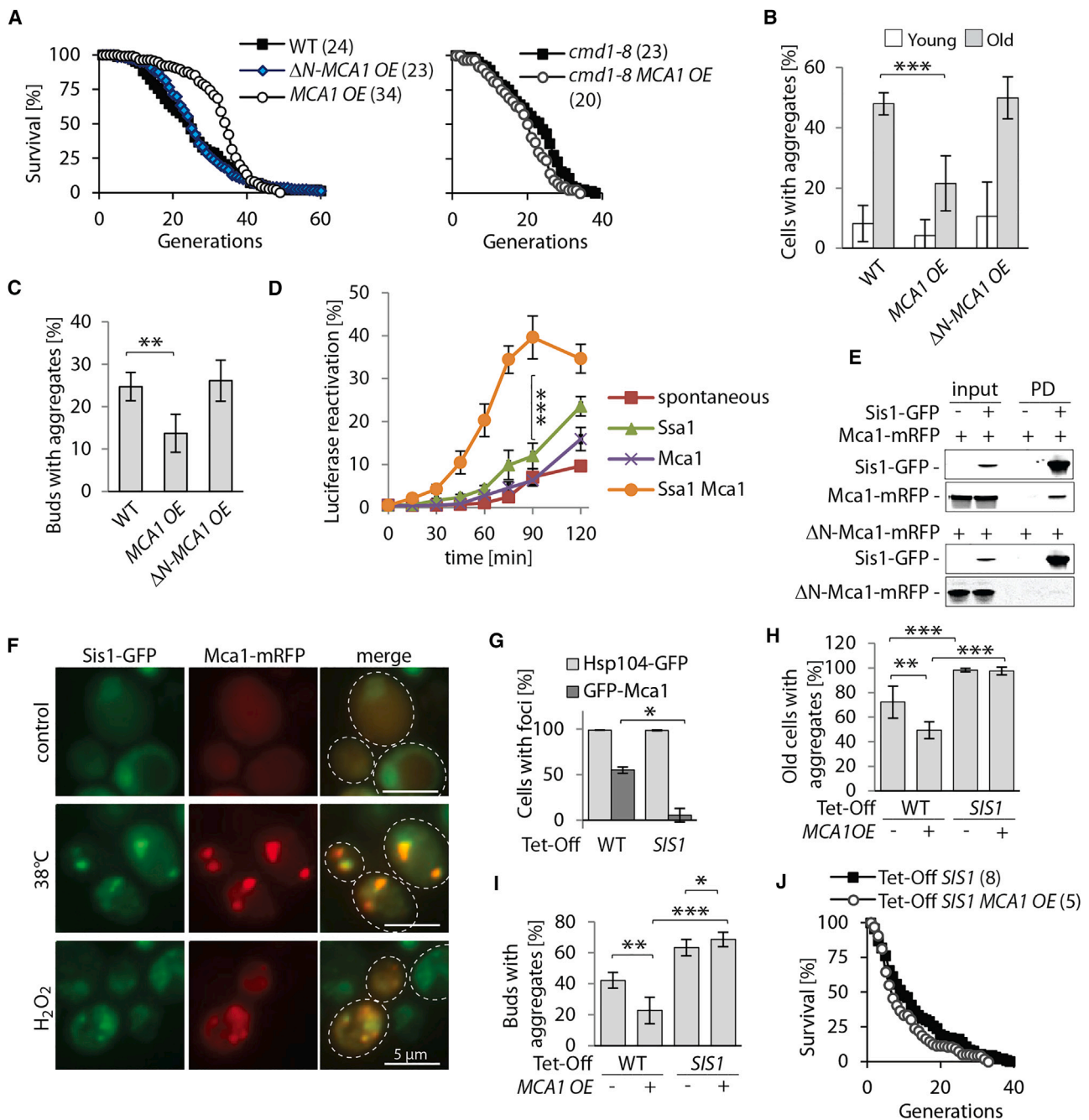
Figure 3. Lifespan extension by Mca1 is linked to Sis1-dependent auxiliary co-chaperone rather than proteolytic activity

(A) Replicative lifespan (RLS; median number of generations is displayed in parentheses) of WT cells (164 cells) and cells OE either the full-length Mca1 (*MCA1 OE*, Mann-Whitney U test p < 0.0001; 114 cells) or ΔN-Mca1 (*ΔN-MCA1 OE*, p = 0.3035; 162 cells). Survival curves represent results of three independent experiments. RLS extension by OE *MCA1* is abolished in calmodulin mutant *cmd1-8* (*cmd1-8*, 84 cells, and *cmd1-8 MCA1 OE*, p = 0.0251, 84 cells). Survival curves represent results of two independent experiments.

(B) Hsp104-GFP aggregate formation in young and replicatively aged cells (13–14 generations) OE either the full-length Mca1 or ΔN-Mca1 (unpaired t test, ***p = 0.00025, n = 2 [for Tet-Off WT background] and 4 [for Tet-Off *SIS1* background] independent experiments).

(C) Hsp104-GFP aggregate inheritance in daughters (buds) of replicatively old cells (unpaired t test, **p = 0.0029, n = 3 independent experiments).

(D) Assisted refolding of guanidinium hydrochloride (GdnHCl)-denatured luciferase by different combinations of Ssa1 and Mca1 as indicated. Luminescence of non-denatured enzyme was taken as 100% (Student's t test, ***p < 0.0005, n > 4).

(E) Interaction of Mca1- and ΔN-Mca1-mRFP with Sis1-GFP from yeast cell extracts. Samples were subjected to immunoblot analysis with anti-GFP and anti-Mca1.

(F) Sis1-GFP co-localization with Mca1-mRFP foci formed after heat stress for 60 min at 38°C or treatment with 0.6 mM H_2O_2 for 90 min. Scale bars, 5 μm.

(legend continued on next page)

requirement of the N-terminal domain for Mca1 targeting to protein aggregates,[17] ΔN-Mca1 overexpression, in contrast to Mca1 overexpression, failed to counteract the accumulation of protein aggregates, visualized by imaging the Hsp104-GFP reporter,[18,36–39] during aging (Figure 3B). Overexpression of ΔN-Mca1 also failed to protect daughter cells from inheriting protein aggregates during cytokinesis, a process that is required for daughter cell rejuvenation (Figure 3C). Moreover, overexpression of wild-type Mca1 failed to both extend lifespan (Figure 3A) and boost aggregate asymmetry during cytokinesis (Figure S3A; Hill et al.[16]) in cells carrying the *cmd1-8* allele of calmodulin, which is unable to bind and suppress Mca1 proteolytic activity (Figure 2). Finally, overexpression of catalytically inactive Mca1C276A has previously been shown to prolong lifespan and to prevent aggregate accumulation.[16] Together, these data suggest that a non-proteolytic mechanism linked to the inhibitory effect of calmodulin on Mca1 protease activity underlies Mca1-dependent effects on cell survival and protein aggregate accumulation. We hypothesized that one such mechanism may be linked to Mca1 acting as a buffer against deficiency in chaperone activity.

Mca1-dependent lifespan extension and quality control require the Hsp40 co-chaperone Sis1

Mca1 has previously been shown to compensate for deficiencies in Hsp40 (Ydj1) activity,[16] and we therefore tested whether Mca1 has Hsp70 co-chaperone-like activity, which might explain its beneficial effects on PQC and lifespan. To this end, *in vitro* luciferase refolding assays[40] were performed with purified components, which demonstrated that Mca1 could substitute for an Hsp40 in Hsp70 (Ssa1) chaperone-dependent refolding (Figure 3D). In contrast to proteolytic activity of Mca1, its refolding activity was not inhibited by calmodulin and did not require the catalytic cysteine 276 (Figure S3B). Thus, binding of calmodulin to Mca1 would favor co-chaperone over protease activity. In addition, as also found by Shrestha et al.,[19] Mca1 interacts physically with the Hsp40 Sis1 in an N-terminal-domain-dependent manner (Figure 3E), and both proteins co-localize at aggregates during proteostatic stress (Figure 3F). Mca1 was not required for Sis1 to localize to cytosolic foci during stress (Figure S3C).[41] In contrast, we found that sequestration of Mca1 to such aggregates required Sis1 (Figure 3G) and that reducing accumulation of aggregates in aging cells by overexpression of Mca1 failed in a Sis1-deficient strain (Figure 3H). Likewise, Sis1 deficiency abrogated the enhancement of asymmetrical segregation of protein aggregates by Mca1 overexpression (Figure 3I). However, we could not detect any synergistic effect between recombinant Mca1 and Sis1 proteins in luciferase reactivation assay (Figure S3D). Finally, Mca1-dependent replicative lifespan extension did not occur in cells with reduced levels of Sis1 (Figure 3J, cf. Figure 3A). Therefore, we conclude that the role of Mca1 in proteostasis and longevity relies on its co-chaperone-like activity and cooperative action with the Hsp40 co-chaperone Sis1.

Constitutive activation of Mca1 protease causes Sis1 cleavage

The Sis1 co-chaperone has previously been shown to be processed into discrete fragments upon purification.[42,43] We found that cleavage of Sis1, but not Ydj1, occurs during replicative aging *in vivo* and is more pronounced in cells carrying the *cmd1-8* allele, where Mca1's proteolytic activation is derepressed (Figures 4A and S4A). Enhanced cleavage of Sis1 was also seen in young cells harboring constitutively active ΔN-Mca1, and this was abolished by the mutation of the catalytic cysteine 276 (Figures 4B and S4B). In addition, we observed that Mca1 cleaved Sis1 in a Ca^{2+}-dependent manner *in vitro* into fragments corresponding in size to those detected *in vivo* (Figure 4C, cf. Figure 4A). In agreement with *in vivo* data, Sis1 cleavage was accelerated by co-incubation with ΔN-Mca1 (Figure 4C). Finally, CaM suppressed the cleavage (Figure 4D). These data further point to dual, and antagonistic, activities of Mca1: as an auxiliary positive factor in Sis1-dependent PQC and longevity assurance and as a protease executing Sis1 cleavage and cell death. Moreover, our data establish calmodulin binding to the N terminus of Mca1 as a *bona fide* mechanism constituting a molecular switch between the two antagonistic activities of the yeast metacaspase.

DISCUSSION

We show here that calmodulin interacts with the QQXX repeats region in the N terminus of Mca1, thus representing a modality of a Ca^{2+}-independent recruitment of calmodulin to a target protein.[31] The fact that calmodulin binds this region *in vitro* provided the impetus to test to what extent such a binding is relevant *in vivo* in the control of Mca1 activity. To wit, our analysis of calmodulin binding to native, full-length Mca1 provides mechanistic and molecular insights reconciling the opposing views of Mca1 as being a cell killer or a protector. We show that Mca1 can act as an inhibitor of growth and executioner of cell death but is normally prevented from doing so by calmodulin binding to its N-terminal pro-domain, which inhibits autocatalytic activation of the protease (Figure 4E). Notably, the activation of Mca1 is not by itself sufficient to trigger cell death and growth arrest since cells harboring ΔN-Mca1 do not display growth defects or increased cell death. Thus, cytological stress/defects displayed by *cmd1* mutants might be additional prerequisites for triggering Mca1-dependent cell death and

(G) Effects of reducing Sis1 levels (*Tet-Off SIS1*) on the formation of Hsp104-associated aggregates and the recruitment of GFP-Mca1 to aggregates (*foci*) following incubation at 38°C for 90 min (unpaired t test, **p < 0.05, n = 2 independent experiments).

(H) Effect of Sis1 level on Mca1-dependent reduction of Hsp104-associated aggregate (*foci*) formation in replicatively old cells (unpaired t test, **p < 0.05 and ***p < 0.005, n = 3 independent experiments).

(I) Effect of Sis1 level on Mca1-dependent reduction of aggregate inheritance by daughter cells (*buds*) after 90 min heat shock at 38°C (unpaired t test, *p < 0.5, **p < 0.05, and ***p < 0.005, n = 2 independent experiments).

(J) Loss of replicative lifespan extension upon Mca1 overexpression with reduced levels of Sis1 (Tet-Off *SIS1*; 93 cells, Tet-Off *SIS1 MCA1* OE; 96 cells, Mann-Whitney U test p = 0.0524) (median number of generations is displayed in parentheses). Survival curves represent results of two independent experiments.
Error bars in (B), (C), and (G)–(I) indicate SD while those in (D) indicate SEM.

Figure 4. Constitutive activation of Mca1 protease causes Sis1 cleavage

(A) Cleavage of Sis1, but not Ydj1, upon replicative aging of WT and *cmd1-8* young (1–4 bud scars) and old (10–14 bud scars) cells. Total cell extracts of isolated cells were subjected to immunoblotting with anti-Sis1 and anti-Ydj1. The unspecific cross-reaction of Sis1 antibody is used as a loading control because Pgk1 runs at the same size as Ydj1 (both mouse antibodies).

(B) Sis1 cleavage in *ΔN-MCA1*-expressing cells displaying constitutive activation of the metacaspase. Of note, we prevented the possibility that released cellular calcium could activate Mca1 during cell lysis by adding 5 mM EGTA to 0.2 N NaOH solution.

(C and D) *In vitro* cleavage of Sis1 by Mca1 and ΔN-Mca1 in the presence of 1 mM CaCl$_2$, and the presence or absence of calmodulin (5 μM CaM, bovine) was monitored by immunoblotting with anti-Sis1.

(E) Model for regulation of Mca1 as either a cytoprotector or cell-death executioner. Calmodulin binding to N-terminal domain of Mca1 protects it from being autocatalytically activated, turning it into a co-chaperone-like cytoprotector acting together with the Hsp40 co-chaperone Sis1. PQC, protein quality control.

growth arrest (Figures 2D–2G).[31] Therefore, it would be interesting to determine whether the stressors previously reported to induce Mca1-dependent cell death[9,12,44,45] affect Cmd1-dependent processes. Since calmodulin binds to and regulates a multitude of protein targets, many different cellular functions, for example cytoskeletal organization, are debilitated in calmodulin-deficient cells, which may make such cells prone to enter a cell-death pathway.[31]

Calmodulin binding to Mca1 would allow the metacaspase to predominantly work as a co-chaperone, and we show that the role of Mca1 in PQC is dependent on the Hsp40 co-chaperone Sis1. In contrast, constitutive activation of Mca1 protease results in Sis1 fragmentation, both *in vivo* and *in vitro*, further indicating that activated Mca1 is unfavorable for cellular PQC (Figure 4E). However, the molecular mechanism whereby Mca1-dependent cleavage of Sis1 contributes to cell death remains unclear. Yet,

Sis1 cleavage might regulate its spatiotemporal co-chaperone activity, and Sis1 mutant proteins lacking their C termini have been found to be neither able to localize to protein deposits/quality control compartments (INQ/JUNQ and IPOD) nor to assist in Hsp104-dependent disaggregation.[46,47]

Calmodulin has been highly conserved throughout evolution and might play a phylogenetically broader, cross-kingdom role in the regulation of longevity in both unicellular and multicellular organisms. Interestingly, there is genetic evidence for a calmodulin-dependent kinase UNC-43, a homolog of human CaMKII, acting together with calcineurin in the regulation of the transcription factor DAF-16, a homolog of human FOXO-3, leading to the activation of a network of genes promoting longevity in *Caenorhabditis elegans*.[48] Furthermore, a similar mechanism appears to operate for regulating transcriptional activity of FOXO-3 in human cells.[48] Whether and how metacaspases, together with calmodulin, are involved in the regulation of aging through the CaMKII/calcineurin pathway in non-animal organisms are questions for future studies.

In summary, Mca1 is involved in replicative lifespan extension as an auxiliary co-chaperone-like factor in a Sis1-dependent manner that does not require protease activity. Calmodulin, by binding to the N-terminal pro-domain of Mca1, favors such co-chaperone-like activity, whereas the absence of calmodulin binding favors Mca1 zymogen-to-active protease transition. Thus, our results establish calmodulin binding to the yeast metacaspase Mca1 as a molecular switch evolved for cellular life and death control. Further research will define whether a similar mechanism is evolutionarily conserved to modulate multifunctional behavior of animal caspases or metacaspases from other eukaryotic lineages.

Limitations of the study

The data on the role of Mca1 in PQC do not reveal the exact biochemical mechanism through which Mca1 acts on protein aggregates. While Mca1 can substitute, *in vitro*, for an Hsp40 protein, including Sis1, in the refolding of luciferase, how the metacaspase speeds up Hsp104/Hsp70/Hsp40-dependent disaggregation *in vivo* is not clear.[16]

Additionally, the results do not pinpoint the exact mechanisms behind Mca1-dependent cell death during stress and in stationary phase, as all possible targets of Mca1-dependent proteolysis, *in vivo*, have yet to be determined under relevant conditions. Moreover, at present, it cannot be ruled out that the increased survival observed when removing *MCA1*, and/or inhibiting its proteolytic activity, is due to compensatory responses. As it is known that many stress defense genes are upregulated upon the removal of *MCA1*,[13] increased survival could be due to a bypass suppression mechanism that overcompensates for the lack of Mca1.

STAR★METHODS

Detailed methods are provided in the online version of this paper and include the following:

- KEY RESOURCES TABLE
- RESOURCE AVAILABILITY

  - ○ Lead contact
  - ○ Materials availability
  - ○ Data and code availability
- EXPERIMENTAL MODEL AND SUBJECT DETAILS
  - ○ Yeast strains
- METHOD DETAILS
  - ○ *E. coli* plasmids
  - ○ Pull down experiments of proteins produced in yeast *S. cerevisiae*
  - ○ Pulldown experiments with proteins produced in *E. coli*
  - ○ Old cells isolation
  - ○ Total cell extracts
  - ○ Immunoblot analysis
  - ○ Lifespan analysis
  - ○ Purification of Mca1 variants, Ssa1, Sis1 and Cmd1 from *E. coli*
  - ○ Firefly luciferase renaturation assay
  - ○ *In vitro* proteolysis by Mca1
  - ○ *In vitro* proteolysis of peptide substrate by Mca1
  - ○ Mass spectrometry analysis of Mca1 *neo* N-termini
  - ○ Labeling with tandem mass tag (TMT) and trypsin digestion
  - ○ nLC-MS/MS
  - ○ Data analysis
  - ○ Growth analysis using spot tests
  - ○ TUNEL assay
  - ○ Clonogenic assay and PI staining of chronologically aged cells
  - ○ Microscopy
- QUANTIFICATION AND STATISTICAL ANALYSIS

INCLUSION AND DIVERSITY

We support inclusive, diverse, and equitable conduct of research.

REFERENCES

1. Yuan, J., and Horvitz, H.R. (2004). A first insight into the molecular mechanisms of apoptosis. Cell *116*, 53–56, 1 p following S59. https://doi.org/10.1016/s0092-8674(04)00028-5.

2. Kumar, S. (2007). Caspase function in programmed cell death. Cell Death Differ. *14*, 32–43. https://doi.org/10.1038/sj.cdd.4402060.

3. Tsiatsiani, L., Van Breusegem, F., Gallois, P., Zavialov, A., Lam, E., and Bozhkov, P.V. (2011). Metacaspases. Cell Death Differ. *18*, 1279–1288. https://doi.org/10.1038/cdd.2011.66.

4. Minina, E.A., Staal, J., Alvarez, V.E., Berges, J.A., Berman-Frank, I., Beyaert, R., Bidle, K.D., Bornancin, F., Casanova, M., Cazzulo, J.J., et al. (2020). Classification and Nomenclature of Metacaspases and Paracaspases: No More Confusion with Caspases. Mol. Cell *77*, 927–929. https://doi.org/10.1016/j.molcel.2019.12.020.

5. Uren, A.G., O'Rourke, K., Aravind, L.A., Pisabarro, M.T., Seshagiri, S., Koonin, E.V., and Dixit, V.M. (2000). Identification of paracaspases and metacaspases: Two ancient families of caspase-like proteins, one of which plays a key role in MALT lymphoma. Mol. Cell *6*, 961–967. https://doi.org/10.1016/s1097-2765(05)00086-9.

6. Vercammen, D., van de Cotte, B., De Jaeger, G., Eeckhout, D., Casteels, P., Vandepoele, K., Vandenberghe, I., Van Beeumen, J., Inzé, D., and Van Breusegem, F. (2004). Type II metacaspases Atmc4 and Atmc9 of Arabidopsis thaliana cleave substrates after arginine and lysine. J. Biol. Chem. *279*, 45329–45336. https://doi.org/10.1074/jbc.M406329200.

7. Sundström, J.F., Vaculova, A., Smertenko, A.P., Savenkov, E.I., Golovko, A., Minina, E., Tiwari, B.S., Rodriguez-Nieto, S., Zamyatnin, A.A., Välineva, T., et al. (2009). Tudor staphylococcal nuclease is an evolutionarily conserved component of the programmed cell death degradome. Nat. Cell Biol. *11*, 1347–1354. https://doi.org/10.1038/ncb1979.

8. Carmona-Gutierrez, D., Bauer, M.A., Zimmermann, A., Aguilera, A., Austriaco, N., Ayscough, K., Balzan, R., Bar-Nun, S., Barrientos, A., Belenky, P., et al. (2018). Guidelines and recommendations on yeast cell death nomenclature. Microb. Cell *5*, 4–31. https://doi.org/10.15698/mic2018.01.607.

9. Madeo, F., Herker, E., Maldener, C., Wissing, S., Lächelt, S., Herlan, M., Fehr, M., Lauber, K., Sigrist, S.J., Wesselborg, S., and Fröhlich, K.U. (2002). A Caspase-Related Protease Regulates Apoptosis in Yeast. Mol. Cell *9*, 911–917. https://doi.org/10.1016/S1097-2765(02)00501-4.

10. Madeo, F., Carmona-Gutierrez, D., Ring, J., Büttner, S., Eisenberg, T., and Kroemer, G. (2009). Caspase-dependent and caspase-independent cell death pathways in yeast. Biochem. Biophys. Res. Commun. *382*, 227–231. https://doi.org/10.1016/j.bbrc.2009.02.117.

11. Hill, S.M., and Nyström, T. (2015). The dual role of a yeast metacaspase: What doesn't kill you makes you stronger. Bioessays *37*, 525–531. https://doi.org/10.1002/bies.201400208.

12. Khan, M.A., Chock, P.B., and Stadtman E, R. (2005). Knockout of caspase-like gene, YCA1, abrogates apoptosis and elevates oxidized proteins in Saccharomyces cerevisiae. Proc Natl Acad Sci U S A *102*, 17326–31. https://doi.org/10.1073/pnas.0508120102.

13. Lee, R.E.C., Puente, L.G., Kærn, M., and Megeney, L.A. (2008). A non-death role of the yeast metacaspase: Yca1p alters cell cycle dynamics. PLoS One *3*, e2956–e2959. https://doi.org/10.1371/journal.pone.0002956.

14. Shrestha, A., Puente, L.G., Brunette, S., and Megeney, L.A. (2013). The role of Yca1 in proteostasis. Yca1 regulates the composition of the insoluble proteome. J. Proteonomics *81*, 24–30. https://doi.org/10.1016/j.jprot.2013.01.014.

15. Dick, S.A., and Megeney, L.A. (2013). Cell death proteins: An evolutionary role in cellular adaptation before the advent of apoptosis. Bioessays *35*, 974–983. https://doi.org/10.1002/bies.201300052.

16. Hill, S.M., Hao, X., Liu, B., and Nyström, T. (2014). Life-span extension by a metacaspase in the yeast Saccharomyces cerevisiae. Science 84 *344*, 1389–1392. https://doi.org/10.1126/science.1252634.

17. Lee, R.E.C., Brunette, S., Puente, L.G., and Megeney, L.A. (2010). Metacaspase Yca1 is required for clearance of insoluble protein aggregates. Proc. Natl. Acad. Sci. USA *107*, 13348–13353. https://doi.org/10.1073/pnas.1006610107.

18. Fischbach, A., Johns, A., Schneider, K.L., Hao, X., Tessarz, P., and Nyström, T. (2023). Artificial Hsp104-mediated systems for re-localizing protein aggregates. Nat. Commun. *14*, 2663–2714. https://doi.org/10.1038/s41467-023-37706-3.

19. Shrestha, A., Brunette, S., Stanford, W.L., and Megeney, L.A. (2019). The metacaspase Yca1 maintains proteostasis through multiple interactions with the ubiquitin system. Cell Discov. *5*, 6–13. https://doi.org/10.1038/s41421-018-0071-9.

20. Watanabe, N., and Lam, E. (2005). Two Arabidopsis metacaspases AtMCP1b and AtMCP2b are arginine/lysine- specific cysteine proteases and activate apoptosis-like cell death in yeast. J. Biol. Chem. *280*, 14691–14699. https://doi.org/10.1074/jbc.M413527200.

21. Wong, A.H.H., Yan, C., and Shi, Y. (2012). Crystal structure of the yeast metacaspase Yca1. J. Biol. Chem. *287*, 29251–29259. https://doi.org/10.1074/jbc.M112.381806.

22. Watanabe, N., and Lam, E. (2011). Calcium-dependent activation and autolysis of arabidopsis metacaspase 2d. J. Biol. Chem. *286*, 10027–10040. https://doi.org/10.1074/jbc.M110.194340.

23. Verma, S., Dixit, R., and Pandey, K.C. (2016). Cysteine proteases: Modes of activation and future prospects as pharmacological targets. Front. Pharmacol. *7*, 107–112. https://doi.org/10.3389/fphar.2016.00107.

24. Gerendasy, D.D., Herron, S.R., Jennings, P.A., and Sutcliffe, J.G. (1995). Calmodulin stabilizes an amphiphilic α-helix within RC3/neurogranin and GAP-43/neuromodulin only when Ca2+ is absent. J. Biol. Chem. *270*, 6741–6750. https://doi.org/10.1074/jbc.270.12.6741.

25. Yamniuk, A.P., and Vogel, H.J. (2004). Structurally Homologous Binding of Plant Calmodulin Isoforms to the Calmodulin-binding Domain of Vacuolar Calcium-ATPase. J. Biol. Chem. *279*, 7698–7707. https://doi.org/10.1074/jbc.M310763200.

26. Dunlap, T.B., Kirk, J.M., Pena, E.A., Yoder, M.S., and Creamer, T.P. (2013). Thermodynamics of binding by calmodulin correlates with target peptide α-helical propensity. Proteins *81*, 607–612. https://doi.org/10.1002/prot.24215.

27. Song, J., Yang, Q., Yang, J., Larsson, L., Hao, X., Zhu, X., Malmgren-Hill, S., Cvijovic, M., Fernandez-Rodriguez, J., Grantham, J., et al. (2014). Essential Genetic Interactors of SIR2 Required for Spatial Sequestration and Asymmetrical Inheritance of Protein Aggregates. PLoS Genet. *10*, e1004539. https://doi.org/10.1371/journal.pgen.1004539.

28. Keinan, E., Abraham, A.C., Cohen, A., Alexandrov, A.I., Mintz, R., Cohen, M., Reichmann, D., Kaganovich, D., and Nahmias, Y. (2018). High-Reynolds Microfluidic Sorting of Large Yeast Populations. Sci. Rep. *8*, 13739–13812. https://doi.org/10.1038/s41598-018-31726-6.

29. Ermolova, N., Kramerova, I., and Spencer, M.J. (2015). Autolytic activation of calpain 3 proteinase is facilitated by calmodulin protein. J. Biol. Chem. *290*, 996–1004. https://doi.org/10.1074/jbc.M114.588780.

30. Davis, T.N., and Thorner, J. (1989). Vertebrate and yeast calmodulin, despite significant sequence divergence, are functionally interchangeable. Proc. Natl. Acad. Sci. USA *86*, 7909–7913. https://doi.org/10.1073/pnas.86.20.7909.

31. Cyert, M.S. (2001). Genetic analysis of calmodulin and its targets in Saccharomyces cerevisiae. Annu. Rev. Genet. *35*, 647–672. https://doi.org/10.1146/annurev.genet.35.102401.091302.

32. Davis, T.N., Urdea, M.S., Masiarz, F.R., and Thorner, J. (1986). Isolation of the yeast calmodulin gene: calmodulin is an essential protein. Cell Nov *47*, 423–431. https://doi.org/10.1016/0092-8674(86)90599-4.

33. Branco, P., Francisco, D., Chambon, C., Hébraud, M., Arneborg, N., Almeida, M.G., Caldeira, J., and Albergaria, H. (2014). Identification of novel GAPDH-derived antimicrobial peptides secreted by Saccharomyces cerevisiae and involved in wine microbial interactions. Appl. Microbiol. Biotechnol. *98*, 843–853. https://doi.org/10.1007/s00253-013-5411-y.

34. Zhu, G., and Davis, T.N. (1998). The fork head transcription factor Hcm1p participates in the regulation of SPC110, which encodes the calmodulin-binding protein in the yeast spindle pole body. Biochim. Biophys. Acta *1448*, 236–244. https://doi.org/10.1016/S0167-4889(98)00135-9.

35. Brockerhoff, S.E., Stevens, R.C., and Davis, T.N. (1994). The unconventional myosin, Myo2p, is a calmodulin target at sites of cell growth in Saccharomyces cerevisiae. J. Cell Biol. *124*, 315–323. https://doi.org/10.1083/jcb.124.3.315.

36. Liu, B., Larsson, L., Caballero, A., Hao, X., Öling, D., Grantham, J., and Nyström, T. (2010). The Polarisome Is Required for Segregation and Retrograde Transport of Protein Aggregates. Cell *140*, 257–267. https://doi.org/10.1016/j.cell.2009.12.031.

37. Liu, B., Larsson, L., Franssens, V., Hao, X., Hill, S.M., Andersson, V., Höglund, D., Song, J., Yang, X., Öling, D., et al. (2011). Segregation of protein aggregates involves actin and the polarity machinery. Cell *147*, 959–961. https://doi.org/10.1016/j.cell.2011.11.018.

38. Erjavec, N., Larsson, L., Grantham, J., and Nyström, T. (2007). Accelerated aging and failure to segregate damaged proteins in Sir2 mutants can be suppressed by overproducing the protein aggregation-remodeling factor Hsp104p. Genes Dev. *21*, 2410–2421. https://doi.org/10.1101/gad.439307.

39. Hanzén, S., Vielfort, K., Yang, J., Roger, F., Andersson, V., Zamarbide-Forés, S., Andersson, R., Malm, L., Palais, G., Biteau, B., et al. (2016). Lifespan Control by Redox-Dependent Recruitment of Chaperones to Misfolded Proteins. Cell *166*, 140–151. https://doi.org/10.1016/j.cell.2016.05.006.

40. Lu, Z., and Cyr, D.M. (1998). The conserved carboxyl terminus and zinc finger-like domain of the co- chaperone Ydj1 assist Hsp70 in protein folding. J. Biol. Chem. *273*, 5970–5978. https://doi.org/10.1074/jbc.273.10.5970.

41. Feder, Z.A., Ali, A., Singh, A., Krakowiak, J., Zheng, X., Bindokas, V.P., Wolfgeher, D., Kron, S.J., and Pincus, D. (2021). Subcellular localization of the J-protein Sis1 regulates the heat shock response. J. Cell Biol. *220*, e202005165. https://doi.org/10.1083/JCB.202005165.

42. Luke, M.M., Sutton, A., and Arndt, K.T. (1991). Characterization of SIS1, a Saccharomyces cerevisiae homologue of bacterial dnaJ proteins. J. Cell Biol. *114*, 623–638. https://doi.org/10.1083/jcb.114.4.623.

43. Yan, W., and Craig, E.A. (1999). The Glycine-Phenylalanine-Rich Region Determines the Specificity of the Yeast Hsp40 Sis1. Mol. Cell Biol. *19*, 7751–7758. https://doi.org/10.1128/mcb.19.11.7751.

44. Guaragnella, N., Pereira, C., Sousa, M.J., Antonacci, L., Passarella, S., Côrte-Real, M., Marra, E., and Giannattasio, S. (2006). YCA1 participates in the acetic acid induced yeast programmed cell death also in a manner unrelated to its caspase-like activity. FEBS Lett. *580*, 6880–6884. https://doi.org/10.1016/j.febslet.2006.11.050.

45. Ludovico, P., Sousa, M.J., Silva, M.T., Leão, C.L., and Côrte-Real, M. (2001). Saccharomyces cerevisiae commits to a programmed cell death process in response to acetic acid. Microbiology *147*, 2409–2415. https://doi.org/10.1099/00221287-147-9-2409.

46. Malinovska, L., Kroschwald, S., Munder, M.C., Richter, D., and Alberti, S. (2012 Aug). Molecular chaperones and stress-inducible protein-sorting factors coordinate the spatiotemporal distribution of protein aggregates. Mol Biol Cell *23* (*16*), 3041–3056. https://doi.org/10.1091/mbc.E12-03-0194.

47. Killian, A.N., and Hines, J.K. (2018 Jan 4). Chaperone functional specificity promotes yeast prion diversity. PLoS Pathog *14* (*1*), e1006695. https://doi.org/10.1371/journal.ppat.1006695.

48. Tao, L., Xie, Q., Ding, Y.H., Li, S.T., Peng, S., Zhang, Y.P., Tan, D., Yuan, Z., and Dong, M.Q. (2013). CAMKII and calcineurin regulate the lifespan of Caenorhabditis elegans through the FOXO transcription factor DAF-16. Elife *2013*, e00518–e00523. https://doi.org/10.7554/eLife.00518.

49. Schneider, C.A., Rasband, W.S., and Eliceiri, K.W. (2012 Jul). NIH Image to ImageJ: 25 years of image analysis. Nat Methods *9* (*7*), 671–675. https://doi.org/10.1038/nmeth.2089.

50. Sambrook, J., Fritsch, E.R., and Maniatis, T. (1989). Molecular Cloning: A Laboratory Manual. In Cold Spring Harb, 2nd ed. (Lab. Press).

51. Erhardt, M., Wegrzyn, R.D., and Deuerling, E. (2010). Extra N-terminal residues have a profound effect on the aggregation properties of the potential yeast prion protein Mca1. PLoS One *5*, e9929. https://doi.org/10.1371/journal.pone.0009929.

52. Janke, C., Magiera, M.M., Rathfelder, N., Taxis, C., Reber, S., Maekawa, H., Moreno-Borchart, A., Doenges, G., Schwob, E., Schiebel, E., and Knop, M. (2004). A versatile toolbox for PCR-based tagging of yeast genes: New fluorescent proteins, more markers and promoter substitution cassettes. Yeast *21*, 947–962. https://doi.org/10.1002/yea.1142.

53. Pfirrmann, T., Lokapally, A., Andréasson, C., Ljungdahl, P., and Hollemann, T. (2013). SOMA: A Single Oligonucleotide Mutagenesis and Cloning Approach. PLoS One *8*, 1–7. https://doi.org/10.1371/journal.pone.0064870.

54. Hwang, C.S., Shemorry, A., and Varshavsky, A. (2009). Two proteolytic pathways regulate DNA repair by cotargeting the Mgt1 alkylguanine transferase. Proc. Natl. Acad. Sci. USA *106*, 2142–2147. https://doi.org/10.1073/pnas.0812316106.

55. Kushnirov, V.V. (2000). Rapid and reliable protein extraction from yeast. Yeast *16*, 857–860. https://doi.org/10.1002/1097-0061(20000630)16:9<857::AID-YEA561>3.0.CO;2-B.

56. Egilmez, N.K., Chen, J.B., and Jazwinski, S.M. (1990). Preparation and partial characterization of old yeast cells. J. Gerontol. *45*, B9–B17. https://doi.org/10.1093/geronj/45.1.B9.

57. Kennedy, B.K., Austriaco, N.R., and Guarente, L. (1994). Daughter cells of Saccharomyces cerevisiae from old mothers display a reduced life span. J. Cell Biol. *127*, 1985–1993. https://doi.org/10.1083/jcb.127.6.1985.

58. Widlund, P.O., Podolski, M., Reber, S., Alper, J., Storch, M., Hyman, A.A., Howard, J., and Drechsel, D.N. (2012). One-step purification of assembly-competent tubulin from diverse eukaryotic sources. Mol. Biol. Cell *23*, 4393–4401. https://doi.org/10.1091/mbc.E12-06-0444.

59. Öling, D., Eisele, F., Kvint, K., and Nyström, T. (2014). Opposing roles of Ubp3-dependent deubiquitination regulate replicative life span and heat resistance. EMBO J. *33*, 747–761. https://doi.org/10.1002/embj.201386822.

60. Zhang, N.-N., Dudgeon, D.D., Paliwal, S., Levchenko, A., Grote, E., and Cunningham, K.W. (2006). Multiple Signaling Pathways Regulate Yeast Cell Death during the Response to Mating Pheromones. Mol. Biol. Cell *17*, 3409–3422. https://doi.org/10.1091/mbc.e06-03-0177.

61. Hu, J., Wei, M., Mirisola, M.G., and Longo, V.D. (2013). Assessing chronological Aging in Saccharomyces cerevisiae. Methods Mol. Biol. *965*, 463–472. https://doi.org/10.1007/978-1-62703-239-1_30.

CellPress
OPEN ACCESS

STAR★METHODS

KEY RESOURCES TABLE

REAGENT or RESOURCE	SOURCE	IDENTIFIER
Antibodies		
Mouse monoclonal anti-GFP	Roche	Roche Cat# 11814460001; RRID: AB_390913
Rabbit polyclonal anti-yeast Mca1	Ekhardt et al., 2010	Gift from Elke Deuerling, Konstanz
Mouse monoclonal anti-6xHis (HIS.H8)	Thermo Fisher	Thermo Fisher Scientific Cat# MA1-21315; RRID: AB_557403
Rabbit polyclonal anti-yeast Sis1	Cosmo Bio	Cosmo Bio Cat# COP-COP-080051; RRID: AB_10709957
Mouse monoclonal anti-Ydj1, clone 1G10.H8	Sigma-Aldrich (MERCK), SAB5200007	Similar to Abnova Cat# MAB2200; RRID: AB_1708336
Rabbit polyclonal anti-GFP	Abcam	Cat# ab6556; RRID: AB_305564
Goat anti-Mouse IRDye 800CW	LI-COR	LI-COR Biosciences Cat# 926–32210; RRID: AB_621842
Goat anti-Mouse IRDye 680RD	LI-COR	LI-COR Biosciences Cat# 926–68070; RRID: AB_10956588
Goat anti-Rabbit IRDye 800CW	LI-COR	LI-COR Biosciences Cat# 926–32211; RRID: AB_621843
Goat anti-Rabbit IRDye 680RD	LI-COR	LI-COR Biosciences Cat# 926–68071; RRID: AB_10956166
Ac-Val-Arg-Pro-Arg-AMC (VRPR-AMC)	BACHEM	4048494
Ac-Asp-Glu-Val-Asp-AMC (DEVD-AMC)	BACHEM	4026262
Bacterial and virus strains		
One Shot™ BL21 Star™ (DE3) Chemically Competent *E. coli*	Invitrogen	C601003
DH5α Competent Cells (*E. coli*)	Invitrogen	EC0112
Chemicals, peptides, and recombinant proteins		
ChromoTek GFP-Trap ® Agarose	Chromotec (Proteintech)	gta-100
cOmplete™ protease inhibitor cocktail	Roche	11697498001
Pefablock SC (AEBSF)	Roche	11429868001
Doxycycline	Sigma-Aldrich	D3447 https://www.sigmaaldrich.com/SE/en/product/sigma/d3447
2-Mercaptoethanol	Sigma-Aldrich	M6250
Wheat Germ Agglutinin Alexa Fluor 555 conjugate (WGA-orange)	Invitrogen	W32464
4-12% gradient 26 well Criterion XT Bis-Tris Protein gel	Bio-Rad	3450125
XT MES running buffer	Bio-Rad	1610789
PVDF membrane	Millipore	IPFL00010
Odyssey Blocking buffer in PBS	LI-COR	927–40000
Eppendorf® LoBind microcentrifuge tubes	Eppendorf	Z666491, Z666505
MagnaBind™ Streptavidin Beads	ThermoFisher	21344
EZ-Link™ Sulfo-NHS-LC-Biotin	ThermoFisher	21335
Caspase-3 human	Sigma-Aldrich	C1224-10UG

Continued

REAGENT or RESOURCE	SOURCE	IDENTIFIER
Calmodulin (human)	ENZO	BML-SE325-0001
Phusion® High-Fidelity DNA Polymerase	NEB	M0530
Taq DNA Ligase	NEB	M0208
T4 DNA Ligase	ThermoFisher	EL0011
QIAprep Spin Miniprep Kit	Qiagen	Cat. No./ID:27206
Pierce™ Trypsin Protease, MS Grade	ThermoFisher	90057
Critical commercial assays		
Pierce™ BCA Protein Assay Kits	ThermoFisher	23227
TMT10plex™ Isobaric Label Reagent Set	ThermoFisher	N/A
Experimental models: Organisms/strains		
S. cerevisiae strain BY4741: Strain background: S288C, genotype: MATa *his3Δ1 leu2Δ0 met15Δ0 ura3Δ0*	EUROSCARF	EUROSCARF: Y00000
All *Saccharomyces cerevisiae* yeast strains used in this study were of the S288C or BY4741 background and are listed in Table S1	EUROSCARF or Nyström laboratory	N/A
S. cerevisiae Yeast Tet-Promoters Hughes Collection (yTHC) strain R1158: Strain background: derived from S288C, genotype: URA3:CMV-tTA MATa his3-1 leu2-0 met15-0	horizon	N/A
Oligonucleotides		
All Oligonucleotides used in this study are listed in Table S2	This paper	Invitrogen
Recombinant DNA		
All plasmids used in this study are listed in Table S3	This study	N/A
Software and algorithms		
ImageJ	(Schneider et al., 2012)[49]	https://imagej.nih.gov/ij/
Other		
Zeiss Axio Observer.Z1 inverted microscope with Apotome and Axiocam 506 camera	Carl Zeiss	N/A
LI-COR Odyssey Infrared scanner	LI-COR	N/A
Criterion Cell	Bio-Rad	1656001
Wet blotting system (Criterion Blotter)	Bio-Rad	1704070
BMG POLARstar Omega microplate reader	BMG LABTECH	N/A

RESOURCE AVAILABILITY

Lead contact
Further information and requests for reagents may be directed to, and will be fulfilled by the Lead Contact, Thomas Nyström (thomas.nystrom@cmb.gu.se).

Materials availability
All unique reagents generated in this study are available from the Lead Contact without restriction.

Data and code availability
- All data reported in this paper will be shared by the lead contact upon request.
- This paper does not report any original code.
- Any additional information required to reanalyze the data reported in this paper is available from the lead contact upon request.

EXPERIMENTAL MODEL AND SUBJECT DETAILS

Yeast strains

Strains, oligonucleotides and plasmids are listed in Tables S1–S3. Media preparation, genetic and molecular biology techniques were carried out using standard methods.[50] Transfmations were done following standard lithium acetate protocol,[16] transformants were confirmed by PCR or immunoblotting. Wild type *MCA1* (432 residues,[51] *MCA1C276A* mutant, and *ΔN-MCA1* (deletion of the first 1–128 amino acids) overexpressors were cloned as previously described.[52] The GPD promoter was amplified from the pYM-N15 plasmid and incorporated upstream the *MCA1* and *ΔN-MCA1* ORF in wild type and *MCA1C276A*.[13] For overexpression and N-terminal tagging with GFP, the pYM-N15 and 17 plasmids were used (Table S3). For *MCA1* knockout, the deletion cassette was amplified from pFA6-natMX4 plasmid (Table S3). pGPD-natNT2-*MCA1C276A* and pGPD-natNT2-*ΔN-MCA1C276A* were amplified (Table S2) and transformed into mutants used in this study (Table S3). Further, *HSP104*-GFP-His3Mx6 was amplified from BY4741 Yeast GFP collection (Invitrogen).

METHOD DETAILS

E. coli plasmids

For construction of pPROEx-HTb-MCA1, MCA1 (1–1299 bases, 432 residues[51] was amplified from yeast *S. cerevisiae* chromosomal DNA with the forward primer 5′-cctaggatccATGTATCCAGGTAGTGGAC-3′ and reverse primer 5′-gctagagctcCTACATAATAAATTGCA GATTTACGTC-3′. PCR product and pPROEx-HT plasmid was digested with SacI and BamHIs HF restriction enzymes prior to ligation. pPROEx-HT-MCA1C276A point mutant, MCA1-Δp10 (amino acids 1–331 of MCA1 ORF) and ΔN-MCA1 (amino acid 129–432) were cloned by the single oligonucleotide mutagenesis and cloning approach (SOMA) as described in.[53] Primers contain the mutation flanked by 25 bp of homologous region 5′-TAGACTAACAGCATTGTTTGACTCTgcTCATTCGGGTACAGTGTTGGATCTT-3′, 5′-TGGTTCTTTAG GTTCTATATTCAAGtagGTTAAGggaGGTATGGGCAATAATG-3′ and 5′-GTATTTTCAGGGCGCCATGGGATCCATGTCTCAATGTACTG GGCGTAGAA-3′ were used, respectively. 50 μL reaction contained 10 μL HF-buffer (NEB), 0.2 mM dNTPs, 0.2 mM phosphorylated primer, 100 ng pPROEx-HT-MCA1 (template DNA), 1 mM NAD+ (SIGMA), 1 μL Phusion (NEB), 1 μL Taq-Ligase (NEB). DNA was denatured 1 min at 95°C, and amplified 30 cycles (1 min 95°C, 1 min 55°C, 4 min 65°C), with 4 min extension time. Afterward 5 μL digestion buffer and 2 μL DpnI were added to fragment the template DNA. Newly synthetized DNA was purified with the PCR purification kit (Qiagen, Hilden) and transformed into *E. coli* (Top 10 competent cells). Mutation was confirmed by sequencing.

Pull down experiments of proteins produced in yeast *S. cerevisiae*

Cells were inoculated and grown overnight in YPD, if carrying pLM1010 (Mca1-mRFP, Mca1 452 residues[13,51]; plasmid in CM-URA selective medium to OD_{600} = 0.7–0.8. Fifty OD_{600} of logarithmically grown cells were harvested and washed twice with ice-cold water (2 min at 3.220xg, 4°C). Cells were washed once with ice-cold IP buffer (115 mM KCl, 5 mM NaCl, 2 mM $MgCl_2$, 1 mM EDTA/NaOH pH 8.0, 20 mM HEPES/KOH pH 7.45) and resuspended in a final volume of 300 μL IP buffer. Cells were snap frozen and kept at −80°C. 200 μL glass beads, 1 mM DTT, 0.5 μg/mL Pefabloc, and 1x cOmplete (Roche) were added (calculated for 1 mL final volume) and cells were lysed by vortexing 10 times for 45 s each with 1 min chilling on ice between the cycles. Lysates were transferred to a new tube and buffer was added to 1 mL final volume. Lysates were incubated with 0.5% Nonidet P-40 (Roche) for 20 min on ice, followed by centrifugation at 16,000xg for 20 min at 4°C. 800 μL of pre-cleared cell lysate was incubated with 20 μL bed volume GFP-TrapA beads (Chromotek) to pull down GFP tagged proteins for 1 h at 4°C on an over-head rotator. Calmodulin Sepharose 4B beads (GE Healthcare) were used to pull down calmodulin interaction partners from cell lysates prepared in IP buffer containing 20 mM EGTA. Beads were pelleted by centrifugation at 2,000 rpm and washed 4 times with respective IP buffer containing 0.5% Nonidet P-40. Beads were boiled for 5 min at 95°C in 2x loading buffer/5% beta-mercaptoethanol prior to immunoblot analysis. IP buffer was adjusted depending on the experiment. 5 mM $CaCl_2$ were added to IP buffer to co-pull down Mca1 with GFP-Cmd1/1–8. 15 mM EGTA were added to co-pull down Mca1 and ΔN-Mca1 with Sis1-GFP.

Pulldown experiments with proteins produced in *E. coli*

His-tagged Mca1 variants were expressed from a plasmid (pRPOEX-HTb-*MCA1/MCA1$_{C276A}$/ΔN-MCA1/MCA1-Δp10*, and the deletions of 11–42, 29–60, 61–78 residues (see Table S3)) in BL21 Star *E. coli*. Overnight cultures were diluted and grown to OD_{600} = 0.1 for 2–3 h at 37°C. Protein expression was induced with 0.5 mM IPTG for 3.5–4 h. Cells were harvested, washed with ice-cold PBS, resuspended in IP buffer (see above) containing 1x cOmplete protease inhibitor (Roche), 0.5 μg/mL Pefabloc, 1 mM DTT, 0.1 mg/mL DNase and 5 mM $CaCl_2$ or 15 mM EGTA, then lysed by tree times exposure to ultrasound for 30 s and chilled for 5 min on ice between the cycles. 0.5% (v/v) Nonidet P-40 was added for 20 min, prior to centrifugation at 16,000xg for 20 min at 4°C. Supernatant was incubated with 20 μL bed volume of Calmodulin Sepharose 4B beads for 1 h at 4°C on an over-head rotator. Beads were washed 4 times with respective buffer/0.5% Nonidet P-40 by centrifugation and processed as described above.

Old cells isolation

Cells were grown overnight to OD_{600} = 0.5–0.6 cell units/ml. 1–3 OD_{600} cells were harvest by centrifugation for 3 min at 3,220xg and washed 3 times with PBS, pH 7.4. Cells were resuspended in 0.8 mL PBS, pH 8.0. 100 μL of freshly prepared 0.005 g/mL Sulfo-NHS-LC Biotin

(Pierce, 0.5mg/sample) were added and cells were shaken at 22°C for 15 min. The cells were washed twice and inoculated in 400 mL YPD overnight. Cells were cooled down on ice, harvested by centrifugation and washed three times as on the previous day but with ice-cold buffer. Cells were resuspended in small volume of PBS (1 mL) and incubated with 10–30 μL of MagnaBind Streptavidin magnetic beads (Thermo scientific) for 30 min at 4°C overhead rotation. Old cells were sorted by a magnet and the daughters were removed by 8 wash steps with PBS, pH 7.4/0.5% (w/v) glucose. Cells were resuspended in fresh medium and grown overnight to allow more divisions. Old cells were isolated by using magnetic beads as on the day before. Cells were further processed for imaging or immunoblot analysis. Replicative age was determined by microscopy using WGA Alexa Fluor 350 (ThermoFisher) to stain bud scars. To deplete Sis1 levels from cells, 2 μg/mL Na-Doxycycline hyclate was added to the cultures.

Total cell extracts
Whole cell extracts were prepared as in.[54,55] Briefly, 1 OD_{600} cell units were harvested and incubated in 0.2 N NaOH complemented with 10 mM EGTA to chelate cellular calcium and cOmplete protease inhibitor (Roche) for 20 min on ice. After spin down at 16,000xg, the pellet was resuspended in 50 μL urea loading buffer (8 M urea in 1x loading buffer as described below, supplemented with 2.5% β-mercaptoethanol). 10–15 μL were used for SDS-PAGE.

Immunoblot analysis
Samples were mixed with loading buffer (4x stock; 200 mM Tris/HCl pH 6.8, 10 mM EDTA/NaOH pH 8.0, 8% (w/v) Na-Dodecyl sulfate (SDS), 20% (v/v) Glycerin, 0.04% (w/v) bromophenol blue, and prior to using 10% (v/v) β-mercaptoethanol was added) followed by boiling for 5 min at 95°C. Proteins were separated by SDS-PAGE (4–12% Criterion XT Bis-Tris; BIORAD) and transferred on Immobilon-FL PVDF membrane (Merck). Primary antibodies (overnight incubation, 4°C) used were rabbit polyclonal anti-Mca1 (gift from E. Deuerling, Germany), rabbit anti-Sis1 (cosmobio), mouse anti-GFP (Roche, clone7.1 and 13.1), rabbit anti-GFP ab290 (Abcam), mouse anti-Pgk1 22C5D6 (Invitrogen), mouse anti-Ydj1 (Sigma, SAB5200007), mouse anti-His (ThermoFisher, HIS.H8), and the secondary antibodies (1h, RT) goat anti-mouse or rabbit with IRDye 680 or 800CW (LI-COR). All antibodies were used in a dilution of 1:20,000 or as indicated. Signal was detected by LI-COR Odyssey scanner. Quantification of protein levels was done with the ImageJ program (NCBI).

Lifespan analysis
Exponentially growing cells were placed on YPD-agar plates. Yeast replicative lifespan was assessed following standard procedures[56,57] by using Singer MSM micromanipulator to select mother cells and remove their daughters. Data were compared by a two-tailed Mann Whitney U test. At least two independent experiments were performed including respective controls. All data shown in the figures were newly generated.

Purification of Mca1 variants, Ssa1, Sis1 and Cmd1 from *E. coli*
Recombinantly expressed Mca1 variants were purified from BL21 Star cells grown in total of 6 L culture. Induction was performed as described above. The following steps were done on ice or 4°C. Cells were harvested by centrifugation at 5,000xg and resuspended in 20 mL HSB3 (50 mM HEPES/NaOH pH 7.45, 300 mM NaCl, 4 mM $MgCl_2$, 20–30 mM imidazole) complemented with 1 mM DTT, 0.5 μg/mL Pefabloc, 1x cOmplete protease inhibitor complex (Roche) and 0.1 mg/mL DNase. Cells were passed 3–4 times through French press (1250 pressure). Lysis was observed under the microscope. Lysates were cleared for 1 h at 100,000xg. Supernatant was incubated with Ni-Sepharose beads (ca 2–4 mL bed volume, GE Healthcare) for 1 h on an over-head rotation incubator. Ni beads were washed 4 times with 25 mL 60 mM imidazole-HSB buffer by short spin at 3,900xg, then three 5-mL elutions with 70 mM, 100 mM, 150 mM, 200 mM imidazole were collected using a Econo column (Bio-Rad). Protein containing fractions were combined and concentrated with Amicon Ultra concentration tube. His tag was cleaved off by incubation with His-TEV protease (Invitrogen). To decrease the imidazole concentration, samples were diluted 10 times with HSB buffer (50 mM HEPES/NaOH pH 7.45, 150 mM NaCl, 4 mM $MgCl_2$), remaining His tagged proteins and contaminations were removed by binding to Ni beads (1–2 mL bed volume) for 1 h and cleaning up by using Econo column. Purified Mca1 variants were concentrated and snap frozen in liquid nitrogen for storage at −80°C.

Sis1, Ssa1 and Cmd1 were purified essentially as Mca1. Briefly, His_6-Sis1 expression was induced from pPROEX-HTb-*SIS1* in total of 1.35 L culture at OD_{600} = 0.3–0.5. 6–8 g wet weight of cells were used to purify Sis1. For Ssa1 or Cmd1 purification His_6-Ssa1/Cmd1 expression was induced at OD_{600} = 0.5 from pPROEX-HTb-*SSA1 or -CMD1* in 2 L culture. After binding the Ni-resin His_6-Ssa1 was washed with HSB buffer containing 50 mM imidazole, first without than once with 50 mM imidazole and 0.5 mM ATP and 0.02% (v/v) Tween 20.[58] Further steps were performed as described above.

Firefly luciferase renaturation assay
230 μM Firefly luciferase (Promega) was dissolved in buffer B1 (25 mM Tris/HOAc pH 7.8, 1 mM EDTA, 1 mM DTT, 0.2 M (($NH_4)_2$)SO_4, 15% Glycerol, 30% ethylene glycol, 2 mM DTT was added to a freshly prepared buffer), aliquoted and kept at −80°C. Luciferase was diluted 20-fold into B1 buffer by incubating 15 min on ice and denatured with GdnHCl (5 M final concentration) and 10 mM DTT at 25°C for 60 min at a final concentration of 2.86 μM in buffer B1. Denatured luciferase was 50-fold diluted into refolding reaction in buffer B2 (50 mM HEPES/KOH pH 7.5, 100 mM KCl, 10 mM Mg(OAc)$_2$, 2 mM DTT freshly added before using B2) containing 5 mM

ATP, 1.6 μM Ssa1 and 3.2 μM Mca1, Mca1C276A, Sis1 and 4 μM calmodulin (ENZO) as specified in the respective figure legends. Renaturation was allowed at 27°C. Luciferase activity was followed over time according to Gold Biotechnology's D-luciferin *in vitro* protocol (USA).[59] Briefly, 3 μL refolding reaction were mixed with 50 μL Luciferase assay buffer (100 mM Tris/HCl pH 7.8, 5 mM MgCl$_2$, 250 μM CoA, 150 μL ATP, 150 μg/l day-luciferin). The luminescence was detected using a POLARstar Omega (BMG Labtech) plate reader. Refolding was calculated as relative value from the native luciferase activity, where luciferase was diluted in buffer B1, without GdnHCl.

In vitro proteolysis by Mca1

Initially calcium-dependent autocleavage of Mca1 was measured in the presence of 50 mM CaCl$_2$ for indicated time at 30°C (HEPES/NaOH pH 7.4, 5 mM DTT, 0.1% CHAPS) (Figure S1). Later, upon optimization of the assay conditions (data not shown), Mca1 auto-processing was inhibited by adding 5 μM human calmodulin (CaM, ENZO) or 2.5 μM Cmd1 in the presence of 1 mM CaCl$_2$ (MES/pH 6, optimal *in vitro* conditions) at RT. Samples were taken as indicated in the figure legends, and used for immunoblot analysis. As control, the respective calmodulin storage buffer was used (CaM-buffer (115 mM KCl, 20 mM HEPES/KOH, pH 7,4, 5 mM NaCl, 2 mM MgCl$_2$, 10% Glycerol), Cmd1-buffer (HBS buffer see above)).

For demonstration of Mca1′s promiscuity, GFP-tagged proteins were pulled-down as described above. Bound proteins were washed twice and resuspended in the reaction buffer and divided equally into 5 tubes. Dependent on the conditions, 1 μM Mca1 and 50 mM CaCl$_2$ were added. Samples were slowly over-head rotated at room temperature (RT) for 2 and 17 h. To assess inhibition of Mca1′s protease activity by calmodulin, Tdh3-GFP (GAPDH) was pulled-down as described above but from 20 OD$_{600}$ yeast cell units. Proteins were eluted two times with 60 μL 200 mM Glycine and neutralized by adding 20 μL 1M Tris/base. 5 μL eluate was processed by adding 1 μM Mca1 in the presence of 5 μM CaM (ENZO, human) in reaction buffer (MES/pH 6 containing 5 mM CaCl$_2$, 5 mM DTT and 0.1% (w/v) CHAPS). To assess Sis1 cleavage by Mca1, purified recombinant Sis1 (0.5 μM) was processed by 0.5 μM Mca1, ΔN-Mca1 and Mca1, in the presence of 2.5 μM human calmodulin (CaM, ENZO) in reaction buffer (50 mM MES/pH 6, 5 mM DTT) in the presence of 1 mM CaCl$_2$ or 20 mM EGTA for indicated time at 25°C.

In vitro proteolysis of peptide substrate by Mca1

50 μM Ac-VRPR-AMC (BACHEM, I-1965-0001) was cleaved in metacaspase reaction buffer (MES/pH 6, 5 mM DTT, 0.1% (w/v) CHAPS) containing 1 mM CaCl$_2$ by adding purified recombinant proteases (1 μM Mca1 variants). Mca1 activity was inhibited by adding 5 μM human calmodulin CaM or 2.5 μM yeast Cmd1 (see above). Proteolytic activity of 0.1 μM Caspase-3 was assessed by using 50 μM Ac-DEVD-AMC in reaction buffer (Tris/pH 7.4, 5 mM DTT; 0.1% (w/v) CHAPS). Time-dependent release of AMC was measured with a BMG Polar Star Omega plate reader (excitation filter 485 nm, emission filter 520 nm). Protease activity was calculated as fluorescent units/min during linear reaction expressed as relative values.

Mass spectrometry analysis of Mca1 *neo* N-termini

5.2 μg Mca1 was autoprocessed by adding 1 mM CaCl$_2$ for 0 min (control) and 60 min at RT (in a total volume of 100 μL). Briefly, the samples were multiplexed and the relative increase of Mca1 *neo* N-termini was detected by mass spectrometry at the proteomics core facility at Gothenburg University. Samples were injected twice to improve data quality. For each sample the average abundance of peptides with the same *neo* N terminus was calculated. The abundance of *neo* N-termini at t = 0 was set to 100%. Noteworthy, this method does not provide the relative abundance of different peptides because of different chemico-physical characteristics/properties during the LC-MS/MS analysis. Thus, we cannot conclude on the hierarchy of cleavage events using this method.

Labeling with tandem mass tag (TMT) and trypsin digestion

Samples were concentrated by vacuum centrifugation to approximately 90 μL. Sodium deoxycholate (SDC, 5%) and triethylammonium bicarbonate (TEAB, 1M) were added to a final concentration of 0.5% SDC and 30 mM TEAB prior to labeling with TMT 10-plex isobaric mass tagging reagents (Thermo Scientific) according to the manufacturer instructions. Samples were combined followed by reduction and alkylation by addition of Tris(2-carboxyethyl)phosphine hydrochloride (TCEP, 5 mM final concentration, 37°C, 30 min) and S-Methyl methanethiosulfonate (MMTS, 10 mM final concentration, RT, 20 min). The multiplexed sample was in-solution digested by addition Pierce MS grade Trypsin (0.15 μg, Thermo Fisher Scientific) in an enzyme to protein ratio of [1:4] at 37°C overnight. An additional portion of trypsin was added and incubated for an extra 3 h. Sodium deoxycholate was removed by acidification with 10% TFA and peptides were desalted using Pierce Peptide Desalting Spin Columns (Thermo Scientific) following the manufacturer's instructions.

nLC-MS/MS

Samples were analyzed on a QExactive HF mass spectrometer interfaced with Easy-nLC1200 liquid chromatography system (Thermo Fisher Scientific). Peptides were trapped on an Acclaim Pepmap 100 C18 trap column (100 μm × 2 cm, particle size 5 μm, Thermo Fischer Scientific) and separated on an in-house packed analytical column (75 μm × 30 cm, particle size 3 μm, Reprosil-Pur C18, Dr. Maisch) using a gradient from 5% to 80% acetonitrile in 0.2% formic acid over 90 min at a flow of 300 nL/min. The instrument operated in data-dependent mode where the precursor ion mass spectra were acquired at a resolution of 60,000, m/z range 400–1600. The 10 most intense ions with charge states 2 to 5 were selected for fragmentation using HCD at stepped collision energy settings of 33. The

isolation window was set to 0.7 Da and dynamic exclusion to 30 s and 10 ppm MS2 spectra were recorded at a resolution of 60 000 with maximum injection time set to 110 ms.

Data analysis

Data analysis was performed using Proteome Discoverer version 2.4 (Thermo Scientific). The database matching was performed using the Mascot search engine v. 2.5.1 (Matrix Science) against a custom database continuing the sequence of the proteins. Precursor mass tolerance was set to 5 ppm and fragment ion tolerance to 30 mmu. Semitrypsin was selected as enzyme with 0 missed cleavages, cysteine methylthiolation was set as fixed modifications and methionine oxidation and TMT10plex on lysine and peptide N-termini was set as a variable modification. Fixed Value for PSM validation and no normalization was used in the search. The reporter ion abundances for the samples were used for evaluation of results.

Growth analysis using spot tests

Cells (5 μL) were spotted on YPD plates in 1–10 dilutions beginning with OD_{600} 0.5 cell units/ml and incubated for 2 days at 30°C.

TUNEL assay

Terminal deoxynucleotidyl transferase dUTP nick end labeling (TUNEL) was performed to detect DNA fragmentation generated during programmed cell death as described in[9,60] with minor modifications. 2×10^7 logarithmically growing yeast cells were harvested and washed three times in PBS. Cells were fixed in 3.7% formaldehyde in PBS for 1 h, washed with PBS and resuspended in 1 mL SPM buffer (1.2 M sorbitol, 50 mM KH_2PO_4/pH 7.3, 1 mM $MgCl_2$). Cell wall was digested with 300 μg/mL zymolyase 100T and 12 μg/mL lyticase for 40 min at 30°C. After washing with SPM buffer (3,220xg, 1 min) cells were resuspended in 50 μL of SPM with 5 μg/mL DNAse-free RNAse (Roche), transferred to a polylysine coated slide and allowed to settle for 20 min at RT. Attached cells were washed three times with PBS and incubated with permeabilization solution (0.1% sodium citrate, 0.1% Trition X-100) for 2 min on ice. Cells were washed twice with PBS prior to 1 h incubation in 50 μL TUNEL reaction mixture (*In Situ* Cell Death Detection Kit, Fluorescein, Roche) at 37°C in humidified atmosphere in the dark. Cells were washed three times with PBS. Mounting media was added to slides and cells were analyzed under fluorescent microscope (EGFP channel). Ratio of TUNEL positive stained cells is based on the average of at least three individual experiments.

Clonogenic assay and PI staining of chronologically aged cells

Clonogenic assay was used to assess chronological aging by counting the fraction of seeded cells which retains the capacity to produce colonies (colony forming units, cfu). Cells were aged as described in CSM supplemented with 0.5% D-Glucose.[61] Cells at day 3 were taken as 100%. Same volume of cells was seeded on YPD plates after 12 days of cultivation. After 3–4 days at 22 °C cfu were counted. To assess the number of dead cells by microscopy, 200 μL of the cell culture was incubated with 1 μL of PI solution (Invitrogen) for 5 min at RT. The proportion of PI stained cells (red channel, see below) was expressed in % of total number of cells imaged by bright-field microscopy.

Microscopy

Images were obtained using Zeiss Axio Observer.Z1-inverted microscope with Axiocam 506 camera, and a Plan-Apochromat 100x/1.40 NA Oil DIC M27 objective (filters 38 HE eGFP in green channel, 45 HQ TexasRed in red channel). Aggregate formation in heat treated cells (90 min at 38°C) or replicatively old cells (see above) was quantified by counting cells displaying Hsp104-GFP foci using ImageJ software and cell-counter plugin. Inheritance was determined as percentage of aggregate-containing buds of total number of buds generated from an aggregate-containing mother cell. For co-localization of Mca1-mRFP with Sis1-GFP, or GFP-Mca1 foci formation 10 mL cultures were grown overnight to 0.5 OD_{600}. Cells were treated with 0.6 mM H_2O_2 or heat-stressed at 38°C for 90 min. Cells were fixed by adding formaldehyde (3.7% final concentration) at RT. After 20 min cells were washed 2 times with PBS. For *SIS1* down regulation cultures were grown with 2 μg/mL Na-Doxycycline hyclate for 22 h.

QUANTIFICATION AND STATISTICAL ANALYSIS

Details about specific statistical tests can be found in the figure legends and respective STAR Methods sections. Lifespan assays were done in three (Figure 3A, WT, *MCA1 OE*, *ΔN-MCA1 OE*) and two (Figure 3A (*cmd1-8*, *cmd1-8 MCA1OE*), Figure 3J) independent experiments. All data points were plotted in one respective graph. Statistical analysis was performed using two-tailed Mann Whitney U test in GraphPad Prism 8.2.1 (Figures 3A and 3J). Quantification of protein levels from Western blot was done with the ImageJ program (NCBI) (Figure 1I). Aggregate and foci formation, PI and TUNEL positive cells, cfu's were quantified using ImageJ software and cell-counter plugin (Figures 2E, 2F, 2G, 3B, 3C, 3G–3I, S3A, and S3C). All data in the bar graphs are presented as an average of n ≥ 3 replicates ±SEM or SD, unless indicated in respective figure legends. In respective figures, asterisks denote statistical significance in p values calculated by unpaired two tailed Student's t test using MS Excel.